

IMPLEMENTATION OF EXTENDED FINITE ELEMENT METHOD IN CRACK PROPAGATION OF CONCRETE

M.R Purba¹, Tulus^{2*}, M.R Syahputra³, Sawaluddin³

^{1,2,3,4}*Program Studi Matematika Fakultas Matematika dan Ilmu Pengetahuan Universitas Sumatera Utara
Medan*

Email : ¹purbamuhammadrafi@gmail.com, ²tulus@usu.ac.id, ³m.romi@usu.ac.id, ⁴sawal@usu.ac.id

Abstract. The Extended Finite Element Method is a numerical solution based on the Finite Element Method (FEM) XFEM has really become a very important generalization of classical finite element techniques, by establishing a mesh independent generalization of classical finite elements to reduce the mesh-dependent shortcomings of the solution. The application of XFEM in crack simulation should improve the modeling of the crack tip environment and also apply to generalized advanced global failure criteria, which is specifically designed to deal with problems in the engineering field Such as the fracture behaviour model. The purpose of this paper is to identify the application of the Extended Finite Element Method to a technical problem, namely fracture behaviour model. The media used is pure boneless concrete modelled with COMSOL Multiphysics 5.6 software by combining stress ratio, lateral strain due to axial loading, concrete density, and crack growth rate. The crack growth process provides initial prolonged growth along with the increase in crack size. In the end, the growth is faster. The reason for this accelerated growth is the stress intensity factor at the crack tip. As the crack grows, the stress intensity factor increases, leading to faster growth. The crack grows until it reaches a critical value, and fracture occurs. The test results obtained the cause of failure: the critical stress intensity is exceeded. See a comparison of crack size and stress cycle as the crack size increases. This accelerated growth is because the growth rate depends on the stress intensity factor at the crack tip, and the stress intensity factor depends on the crack size. As the crack grows, the stress intensity factor increases, leading to faster growth. The crack grows to a critical size, and failure occurs. The results show a relatively strong relationship between increasing crack size and increasing crack growth rate.

Keywords: Engineering field, Crack Growth, Crack Propagation, Extended Finite Element Method

I. INTRODUCTION

Practical application of concrete structures requires extensive research and understanding of the response and behavior of various loads. There are many methods of studying the behavior of concrete structures, including experimental, numerical, and theoretical [1]. Understanding the properties of concrete is essential to avoid errors in concrete structures or repair or retrofitting damaged structures and design errors. Due to cost and time limitations in the study of concrete performance, finite element analysis numerical methods can accurately simulate

the behavior of concrete structures. Finite element analysis used in structural engineering determines the overall behavior of a structure by dividing it into simple elements, each with well-defined mechanical and physical properties [2]. Many commercial finite element analysis software is available, including ABAQUS, COMSOL, ANSYS, NASTRAN, and Hypermesh [3]. COMSOL Multiphysics was used because of its strengths, the comprehensive ability of "COMSOL Multiphysics" to handle the simulation of multi-field problems and its appeal to researchers and engineers that motivated this work to pursue COMSOL's first XFEM implementation. Provides a straightforward approach to the proposed XFEM implementation using built-in functions provided by COMSOL. Structural analysis using these tools proved to be faster and more efficient than experimental analysis [4], [5]. Computational studies of fracture networks are of great interest to engineers working with materials that fracture before they can be plastically deformed. XFEM Can occur when the material is in the "pre-stressed" phase, while these small deformations and strains can cause the material to exceed its critical stress. Of great importance to researchers is the prediction of crack nucleation and the total dependence of the resulting crack pattern on the material properties [6], [7].

Computational methods are increasingly important in modeling cracks in materials. Due to the complex nature of fracture mechanics, several phenomenological methods have been carried out. The method includes the extended finite element method (X-FEM) or an extended method, while this method is included in the Partition of Unity Methods (PUM) [6], [8]. The finite element function space is a function of the discontinuous form, which can model the placement of one of the cracks or the other side of the crack plane. The main advantage lies within each element without continuously interlocking between individual crack meshes. This study presents an experimental analysis of the behavior of pure concrete using the COMSOL Multiphysics 5.6 [9].

II. MATHEMATICAL MODEL

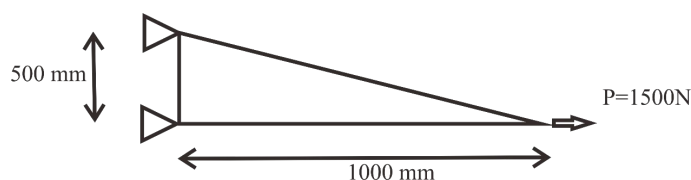


Figure 1. Illustration of Linear Triangle Elements on material

In the extended finite element method for the numerical solution of elliptic partial differential equations, the stiffness matrix represents the system of linear equations that must be solved in order to determine an approximate solution to the differential equation. The Extended Finite Element Method (XFEM) is a numerical solution, which is based on the Finite Element Method (FEM), which is specially designed to deal with problems in engineering (engineering) [10]. Like the fracture behavior ini Ilustration of Linier Triangle Elements model in Figure 1, while the element stiffness matrix or $[k]$ can be calculated as follows,

$$[k]\{d\} = \{r\}$$

$$[k] = \int [B]^T [E] [B] t dA$$

where $\{d\}$ is the horizontal deformation (translation), $\{r\}$ is the load at node, t is the thickness of material, d is the density of material, A is the field of material and ν represents a Poisson ratio. For stiffness matrix $[E]$ and $[B]$ as follows:

$$[E] = \frac{E}{1 - \nu^2} \begin{bmatrix} 1 & \nu & 0 \\ \nu & 1 & 0 \\ 0 & 0 & \frac{1 - \nu}{2} \end{bmatrix}$$

where ν represents the Poisson ratio and

$$[B] = \frac{1}{2A} \begin{bmatrix} \beta_i & 0 & \beta_j & 0 & \beta_k & 0 \\ 0 & \gamma_i & 0 & \gamma_j & 0 & \gamma_k \\ \gamma_i & \beta_i & \gamma_j & \beta_j & \gamma_k & \beta_k \end{bmatrix}, \beta_i = y_i - y_k, \beta_j = y_k - y_i, \beta_k = y_i - y_j, \gamma_i = x_k - x_j, \gamma_j = x_i - x_k, \gamma_k = x_j - x_i.$$

The path of creeping fracture behavior can be analyzed theoretically by applying different fracture mechanics criteria [11]. Crack growth occurs when the maximum tangential stress reaches a critical value, and the degree of the crack in the radial direction corresponds to the maximum tangential stress [12]. The crack tip stress field is close to the isotropic homogeneous linear equation:

COMSOL Multiphysics 5.6 on XFEM separates interfaces, such as cracks or material discontinuities, from the back soil net by enriching the finite element space with a unique enrichment function based on the unitary method partitioning. Therefore, it eliminates the repair steps required in classic movable interface element modeling. In this method, the fractured interface topology and evolution are handled using the node distance to the appropriate projection point on the interface. COMSOL Multiphysics 5.6 can use the Level Set Method (LSM); an extension to higher dimensions with XFEM is straightforward. The special treatment of the Galerkin finite element formulation, described in the following section, facilitates the separation of the weak form from the standard and enriched parts of the equation, which corresponds to the COMSOL Multiphysics modeling structure [13], [14][15].

COMSOL is a numerical simulation software based on the finite element method that COMSOL Multiphysics 5.6 can use for various applications, ranging from modeling civil engineering structures, which laboratory test results can then verify. Standard and Explicit have two primary analyses (using an explicit, active finite element formulation) to model dynamic events [16].

This standard uses the finite element method to implicitly solve any "additional" solution to a system of equations for the analysis of solid, shell, and truss models. COMSOL Multiphysics can use the program to solve static and dynamic problems and a combination of linear and nonlinear problems [17].

COMSOL is a finite element-based computer program used to analyze various nonlinear problems, including reinforced concrete beams and prestressed concrete. The program's capability is unquestionable, as it can accurately unify different element models, bringing them closer to reality and enabling dynamic and cyclic load analysis. COMSOL provides solutions for various constitutive equations to solve nonlinear problems, making it easier for users to choose the right solution for the model to be analyzed. Important part. COMSOL's consistency in software development has resulted in advances in the accuracy of

material modeling, geometry, and load modeling to achieve results that are accurate and close to the real world [18][19].

Essentially, XFEM enriches the finite element space with special enrichment functions based on unit partitioning methods, which decouple boundary surfaces (such as cracks or material discontinuities) from the background mesh. Thus, the remeshing step required for classical finite element modeling of moving interfaces is eliminated. In this method, the processing of crack interface topology and its evolution is done by using the distances of nodes to corresponding projected points on the interface. Alternatively, XFEM can use the Level Set Method (LSM), easily extended to higher dimensions and coupled with XFEM. The specific treatment of Galerkin's finite element formulations is detailed in the next section, helping to differentiate between the standard weak form and the enriched portion of the governing equations that can be used to model structures in COMSOL Multiphysics. [20]

In terms of modeling, COMSOL provides various models to choose from. Users can choose the model according to the test object's geometry, material, and behavior.

III. NUMERICAL RESULT AND DISCUSSION

Before the calculation is carried out, the stress ratio (Young's modulus) is $2.35 \times 10^4 \text{ Mpa}$, the lateral strain due to axial loading (Poisson ratio) is 0.17, and the Concrete Density (Density) is 2.4 g/cm^3 . in the test given a crack growth rate (Paris' law coefficient) of 1.4×10^{-11} , given the specifications of the material tested in the laboratory with specifications: Length 100cm , Width 50cm , Thickness 50mm , and Initial crack initiation by 1cm . in the test found the number of cycles that can be achieved before failure is :

$$N_{fail} = 5.431 \text{ cycles to failure}$$

As the crack increases, the stress intensity factor at the crack tip increases. Failure occurs when the stress intensity factor exceeds the critical stress intensity of the material, namely K_{Ic} .

Table 1 shows the pressure range i that makes up the pressure history. The pressure history is run repeatedly until failure.

Table 1. Tabel *Stress History*

Cycles	Tensile Max	Tensile Min	Bending Max	Bending Min
100	137,9 Mpa	0,000 Mpa	68,85 Mpa	0,000 Mpa
125	68,95 Mpa	34,47 Mpa	0,000 Mpa	0,000 Mpa

The number of cycles in the stress history, N_{hist} , is 125 *cycles*. The number of stress histories that can be repeated before failure is:

$$X_{hist} = \frac{N_{fail}}{N_{hist}} = 43 \text{ history repetitions to failure}$$

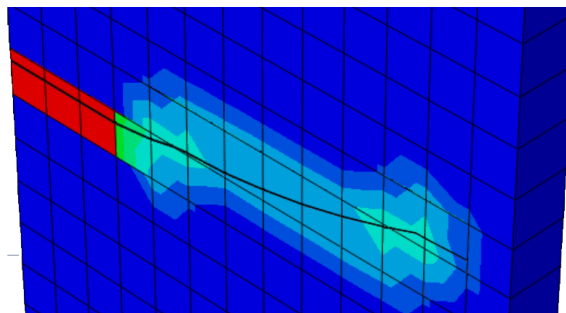


Figure 2. Shape and direction Crack development in the material under test.

Knowing the growth of cracks, crack growth occurs when the energy change must be equal to or exceed the resistance. If the change in energy is less than the change in resistance, cracking will not occur. For the case of voltage, use the maximum voltage value. The maximum stress intensity factor is compared with K_{Ic} to determine failure.

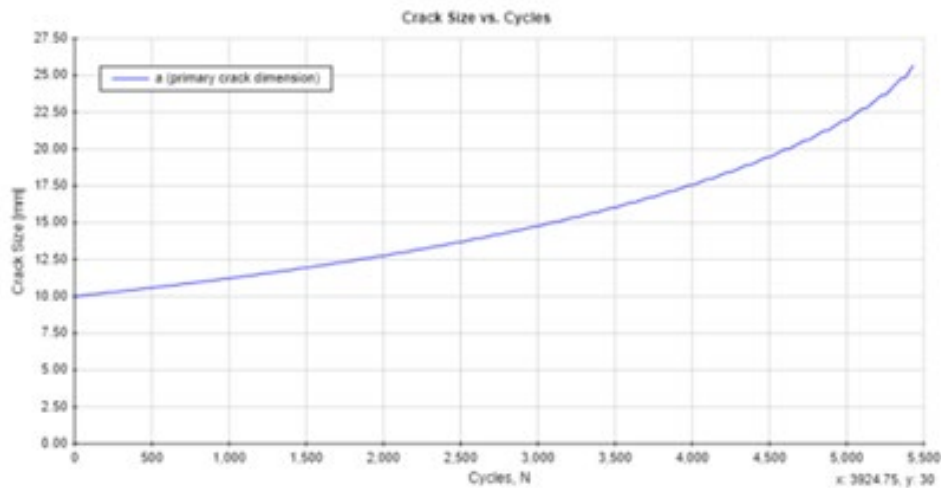


Figure 3. Comparison of crack size with stress cycle.

Stipulations in the crack growth process from Figure 3 can be seen that, at first, the growth was prolonged with an increase in the size of the crack. In the end, the growth was faster $\left(\frac{da}{dN}\right)$. This accelerated growth is the stress intensity factor at the crack tip a . The stress intensity factor increases as the crack grows, leading to faster growth. The crack grows until it reaches a critical value, and fracture occurs.

The test results obtained the cause of failure: the critical stress intensity is exceeded. To see the comparison between the crack size and the stress cycle is shown in Figure 2. As the crack size increases. This accelerated growth is because the growth rate depends on the stress intensity factor at the crack tip, and the stress intensity factor depends on the crack size. The stress intensity factor increases as the crack grows, leading to faster growth. The crack grows to a critical size, and failure occurs. Figure 2 shows the crack size as a function of the stress cycle. The stress intensity factor, K , depends on the size of the crack. The stress intensity increases as the crack increases. Once the crack reaches a critical size (i.e., the crack has developed to the point where the stress intensity equals the critical stress intensity, $K_{critical}$ of the material), the section fractures synchronously.

The fracture toughness depends on the thickness of the part. As the thickness increases, the fracture toughness decreases until the strain-plane fracture toughness K_{Ic}

Figure 4 shows the direction of the crack and the shape of the fracture in the material being tested. The fracture on the material indicates the end of the analysis. The analysis ends in a cycle of 5,431 with a K_{max} of $65.95 \text{ Mpa} \times m^{5 \times 10^{-1}}$ for sampling data from simulation results. Can be seen in Appendix 2 Sampling of Crack Growth Results.

The following numerical simulation results show the application of Finite Element: implementation in calculating crack propagation in complex geometries. In this case, the loading conditions are quasi-cyclic (quasi-static), and the crack propagation angle is determined based on the Stress Intensity Factor (SIF) shown during the simulation; initial geometry initiation with 1575 tetrahedra mesh, crack gap is positioned straight in the center of

the material, where the crack is expected to spread. The fracture equation applied is the Paris Fatigue Law with the hypothesis of maximum circumferential stress for the crack propagation angle in the simulation. The change in crack length for each iteration is considered a constant Δ_a . Numerical results obtained from modeling found on crack development using simulation show crack trajectories and contour stress Von-Misses stress σ_v at the end of the analysis Figure 5 illustrates the material condition and direction of the crack trajectory of concrete at the 2.500 cycles iteration has obtained a crack fracture growth of 0.368 cm with a maximum pressure of $K_{max} = 48.67 \text{ Mpa}$.

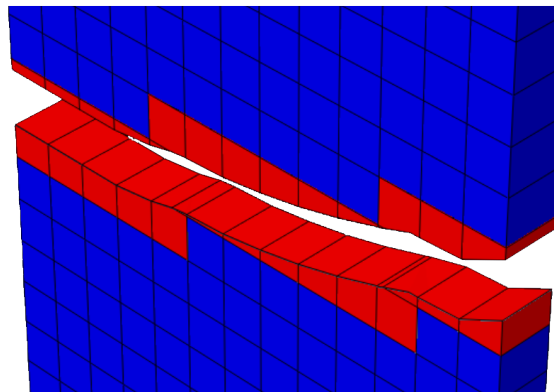


Figure 4. Comparison of crack size with stress cycle.

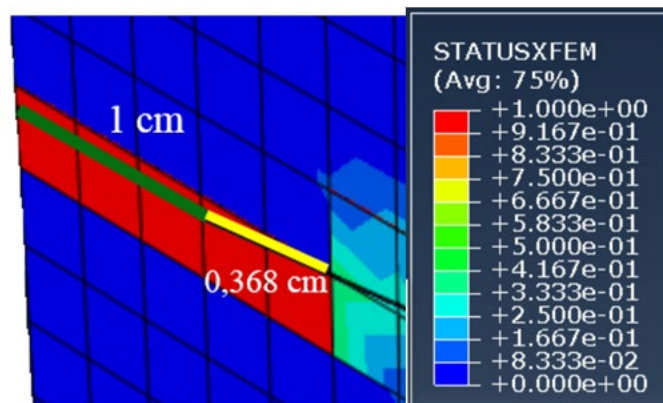


Figure 5. Displacement distribution contour on crack path based on ψ and *Von-Misses* stress σ_v

At the end of the simulated three-dimensional crack test, the cracks were found to be nearly parallel to the surface, the results confirming flexibility in handling more complex scenarios in 3D crack analysis problems. The relationship that occurs in 3D crack analysis is generally node-to-segment, i.e. there will be no pair of overlapping elements, that is, each element does not have more than 1 master segment or slave node to view various crack scenarios.

IV. CONCLUSION

The crack growth rate is obtained from the calculation results on COMSOL Multiphysics 5.6. The crack growth rate is shown as a function of the crack length. With a fairly strong relationship, the increase in cracks from the beginning cracks increases the crack growth rate.

From the constants used in Paris' Law, the crack growth rate is proportional to the stress intensity factor to the power of 3.1. The results show that the stress intensity factor increases strongly with crack length, which increases the crack growth rate.

From the results of this research, the suggestions given by the author for further research are to look at the characteristics of crack behavior in other materials that can provide a lower propagation rate and examine how the influence of different types of concrete models on the crack behavior that occurs.

ACKNOWLEDGMENTS

The author thanks Prof. Tulus., M.Sc., Ph.D. as the supervisor of this research and Muhammad Romi Syahputra., M.Si, and Dr. Sawaluddin., M.IT as the commission for examining this research, and the author would like to thank the reviewers for their comments and suggestions for improving this paper.

REFERENSI

- [1] A. Bergara, J. I. Dorado, A. Martin-Meizoso, dan J. M. Martínez-Esnaola, "Fatigue crack propagation in complex stress fields: Experiments and numerical simulations using the Extended Finite Element Method (XFEM)," *Int. J. Fatigue*, vol. 103, hal. 112–121, 2017, doi: 10.1016/j.ijfatigue.2017.05.026.
- [2] C. Beams, "Modeling the Behavior of CFRP Strengthened Concrete Beams and Columns at," 2020.
- [3] W. Demin dan H. Fukang, "Investigation for plastic damage constitutive models of the concrete material," *Procedia Eng.*, vol. 210, hal. 71–78, 2017, doi: 10.1016/j.proeng.2017.11.050.
- [4] Y. Wang dan H. Waisman, "An arc-length method for controlled cohesive crack propagation using high-order XFEM and Irwin's crack closure integral," *Eng. Fract. Mech.*, vol. 199, no. May, hal. 235–256, 2018, doi: 10.1016/j.engfracmech.2018.05.018.
- [5] K. Tazoe, H. Tanaka, M. Oka, dan G. Yagawa, "An analysis of half elliptical surface crack propagation phenomenon with smoothed particle hydrodynamics method," *5th Int. Conf. Part. Methods - Fundam. Appl. Part. 2017*, hal. 890–897, 2017.
- [6] A. Lisjak, D. Figi, dan G. Grasselli, "Journal of Rock Mechanics and Geotechnical Engineering Fracture development around deep underground excavations: Insights from FDEM modelling," *J. Rock Mech. Geotech. Eng.*, vol. 6, no. 6, hal. 493–505, 2014, doi: 10.1016/j.jrmge.2014.09.003.
- [7] F. L. Sun dan C. Y. Dong, "Three-dimensional crack propagation and inclusion-crack interaction based on IGABEM," *Eng. Anal. Bound. Elem.*, vol. 131, no. April, hal. 1–14, 2021, doi: 10.1016/j.enganabound.2021.06.007.
- [8] X. Xia, F. Chen, X. Gu, N. Fang, dan Q. Zhang, "Interfacial debonding constitutive model and XFEM simulation for mesoscale concrete," *Comput. Struct.*, vol. 242, hal. 106373, 2021, doi: 10.1016/j.compstruc.2020.106373.
- [9] A. M. Singh dan M. M. Sharma, "Analysis on Fatigue Crack Initiation and Fatigue Crack Propagation in a Gear," *Smart Moves J. Ijoscience*, vol. 4, no. 7, hal. 13, 2018, doi: 10.24113/ijoscience.v4i7.155.
- [10] R. Brighenti, M. C. S. Moreno, dan E. Barbieri, *8 - Computational techniques for simulation of damage and failure in composite materials*. Elsevier Ltd, 2015. doi: 10.1016/B978-0-08-100137-0.00008-0.

- [11] H. Dirik dan T. Yalçinkaya, “Crack path and life prediction under mixed mode cyclic variable amplitude loading through XFEM,” *Int. J. Fatigue*, vol. 114, hal. 34–50, 2018, doi: 10.1016/j.ijfatigue.2018.04.026.
- [12] O. N. Stepanova, L., & Belova, “Estimation of crack propagation direction angles under mixed mode loading in linear elastic isotropic materials by generalized fracture mechanics criteria and by molecular dynamics method Estimation of crack propagation direction angles under mixed mode I,” *J. Phys. Conf. Ser.*, vol. 1096, hal. 012060, 2018, doi: 10.1088/1742-6596/1096/1/012060.
- [13] S. Liang, Y. Zhu, M. Huang, dan Z. Li, “Simulation on crack propagation vs. crack-tip dislocation emission by XFEM-based DDD scheme,” *Int. J. Plast.*, vol. 114, no. October 2018, hal. 87–105, 2019, doi: 10.1016/j.ijplas.2018.10.010.
- [14] X. Y. Fang, H. N. Zhang, dan D. W. Ma, “Influence of initial crack on fatigue crack propagation with mixed mode in U71Mn rail subsurface,” *Eng. Fail. Anal.*, vol. 136, no. March, hal. 106220, 2022, doi: 10.1016/j.engfailanal.2022.106220.
- [15] F. Meray, T. Chaise, A. Gravouil, P. Depouhon, B. Descharrieres, dan D. Nélías, “A novel SAM/X-FEM coupling approach for the simulation of 3D fatigue crack growth under rolling contact loading,” *Finite Elem. Anal. Des.*, vol. 206, no. April, hal. 103752, 2022, doi: 10.1016/j.finel.2022.103752.
- [16] Y. Zhang, Z. Gao, Y. Li, dan X. Zhuang, “On the crack opening and energy dissipation in a continuum based disconnected crack model,” *Finite Elem. Anal. Des.*, vol. 170, no. June 2019, hal. 103333, 2020, doi: 10.1016/j.finel.2019.103333.
- [17] Y. Zhang, J. Huang, Y. Yuan, dan H. A. Mang, “Cracking elements method with a dissipation-based arc-length approach,” *Finite Elem. Anal. Des.*, vol. 195, no. March, hal. 103573, 2021, doi: 10.1016/j.finel.2021.103573.
- [18] L. Di Stasio dan Z. Ayadi, “Finite Element solution of the fiber/matrix interface crack problem: Convergence properties and mode mixity of the Virtual Crack Closure Technique,” *Finite Elem. Anal. Des.*, vol. 167, no. July, hal. 103332, 2019, doi: 10.1016/j.finel.2019.103332.
- [19] M. R. Javanmardi dan M. R. Maheri, “Extended finite element method and anisotropic damage plasticity for modelling crack propagation in concrete,” *Finite Elem. Anal. Des.*, vol. 165, no. July, hal. 1–20, 2019, doi: 10.1016/j.finel.2019.07.004.
- [20] A. Jafari, P. Broumand, M. Vahab, dan N. Khalili, “An eXtended Finite Element Method implementation in COMSOL Multiphysics: Solid Mechanics,” *Finite Elem. Anal. Des.*, vol. 202, 2022, doi: 10.1016/j.finel.2021.103707.